Hydrol. Earth Syst. Sci. Discuss., doi:10.5194/hess-2016-380, 2016
Manuscript under review for journal Hydrol. Earth Syst. Sci.
Published: 22 August 2016

Hydrology and Earth System Sciences
Discussions
Open Access
EGU

A systematic examination of the relationship between CDOM and DOC for various inland waters across China

Kaishan Song[1], Ying Zhao[1, 2], Zhidan Wen[1], Jianhang Ma[1, 2], Tiantian Shao[1], Chong Fang[1, 2], Yingxin Shang[1]

[1]Northeast Institute of Geography and Agroecology, CAS, Changchun, 130102, China

[2] University of Chinese Academy of Sciences, Beijing 100049, China

Corresponding author's E-mail: songks@iga.ac.cn; Tel: 86-431-85542364

Abstract: Chromophoric dissolved organic matter (CDOM) plays a vital role in aquatic ecosystems. Strong relationship has been proven between CDOM and dissolved organic carbon (DOC), which set the basis for remote estimation of DOC with remote sensing data. An algorithm has been developed to retrieve DOC via CDOM absorption at 275 and 295 nm with coastal waters. However, the relationship between DOC and $a_{CDOM}(275)$ and $a_{CDOM}(295)$ for different types of inland waters are still not clear. Further, is the relationship stable with different types of inland waters? In the current investigation, samples from fresh lakes, saline lakes, rivers or streams, urban water bodies, ice-covered lakes were examined. The regression model slopes range from 1.03 for urban waters to 3.13 for river water, with extreme low slope value for highly saline waters (slope is about 0.3); while coefficient of determinations (R^2) range from 0.71 (urban waters) to 0.93 (winter waters). The specific CDOM absorption (SUVA254) showed the similar trend, i.e., low values were observed for saline water and waters from semi-arid or arid regions, where strong photo-bleaching

Hydrol. Earth Syst. Sci. Discuss., doi:10.5194/hess-2016-380, 2016
Manuscript under review for journal Hydrol. Earth Syst. Sci.
Published: 22 August 2016

Hydrology and Earth System Sciences
Discussions

is expect due to thin ozone layers, less cloud cover, longer water residence time and sunshine hours. In the contrast, high values were measured with waters developed in wetlands or forest in Northeast China, where inverse environmental settings were witnessed. The investigation also demonstrated that stronger relationships between CDOM and DOC were revealed when CDOM275 were sorted by SUVA254 ($0.78<R^2<0.98$) or the ratio of CDOM250:CDOM365 ($0.78<R^2<0.99$). Our results highlight that non-unified relationship exhibits for different types of inland waters, and remote sensing models for DOC need to be tuned with different inherent optical parameters obtained from various types of waters for quantification of DOC in inland waters.

Keywords: Absorption, CDOM, DOC, spectral slope, saline water, fresh water

1. Introduction

Inland waters play a substantial role for regulating climate at regional scale, and also for global carbon cycling (Cole et al., 2007; Tranvik et al., 2009). Compared with other terrestrial ecosystems, e.g., forest, grassland and agricultural ecosystem, inland waters only occupy a small fraction (3.5%) of the earth surface (Verpoorter et al., 2014). However, they play a disproportional role for global carbon cycling with respect to carbon transportation, transformation and carbon storage (Tranvik et al., 2009; Verpoorter et al., 2014). According to Tranvik et al. (2009), 2.9 Pg C/yr was imported from terrestrial ecosystems to inland waters, of which about 0.6 Pg C was buried in the lake sediment each year, 1.4 Pg C/yr was released into the air as CO_2 or

Hydrol. Earth Syst. Sci. Discuss., doi:10.5194/hess-2016-380, 2016
Manuscript under review for journal Hydrol. Earth Syst. Sci.
Published: 22 August 2016

45 methane, and the rest of 0.9 Pg C/yr was exported to the ocean via river channels.
46 However, the amount of C retained in the inland waters is still not clear or the
47 uncertainty is still remained for the current knowledge (Raymond et al., 2013). It has
48 been proposed by several researchers that remote sensing might provide a promising
49 tool for quantification of various carbon fractions and carbon storage for inland waters
50 (Cole et al., 2007; Tranvik et al., 2009; Song et al., 2013; Kutser et al., 2015).

51 Colored dissolved organic matter (CDOM) is one of the largest bioactive
52 reservoirs at earth's surface (Para et al., 2010), and influences light transmittance in
53 aquatic ecosystems (Vodacek et al., 1997; Williamson and Rose, 2010). Dissolved
54 organic carbon (DOC), the major component of CDOM, is a source of nutrients and
55 energy for heterotrophic bacteria, and the mineralization of allochthonous DOC in the
56 aquatic systems into net source of CO_2 in the atmosphere (Jaffe et al., 2008; Raymond
57 et al., 2013). DOC also serves to mediate the chemical environment through
58 production of organic acids (Landon and Bishop, 2002; Brooks and Lemon, 2007),
59 enhance or alleviate toxicity of heavy metals (Cory et al., 2006). A bunch of
60 researches have been conducted to characterize the spatial and seasonal variations of
61 CDOM and DOC for both inland and oceanic waters (Vodacek et al., 1997; Neff et al.,
62 2006; Stedmon et al., 2011) in ice free season, but less is known about saline lakes
63 (Song et al., 2013; Wen et al., 2016), urban waters influenced by sewage effluent and
64 ice covered waters in winter (Belzile et al., 2000, 2002).

65 The relationship between DOC and CDOM sets a bridge for remote estimation of
66 DOC in both oceanic water (Hoge et al., 1996; Bricaud et al., 2012; Nelson et al.,

Hydrol. Earth Syst. Sci. Discuss., doi:10.5194/hess-2016-380, 2016
Manuscript under review for journal Hydrol. Earth Syst. Sci.
Published: 22 August 2016

2012) and inland waters (Yu et al., 2010; Griffin et al., 2011; Song et al., 2013; Zhu et al., 2013). Thus, various attempts have been made to examine the relationship between DOC and CDOM. According to Fichot and and Benner (2011), close relationship between CDOM and DOC was observed for water from Mexican Gulf, and stable regression model was established between DOC and $a_{CDOM}(275)$ and $a_{CDOM}(295)$. Similar findings also observed in other estuary waters along a salinity gradient, e.g., the Baltic Sea along the Finish Gulf (Kowalczuk et al., 2006), the Chesapeake Bay (Le et al., 2013). However, investigation by Chen et al. (2004) also indicated that the relationship between CDOM and DOC was not conservative due to some process could either be estuarine mixing or photo-degradation. Similar arguments were raised by Spencer et al. (2009) for waters from Congo River and for waters across the mainland of USA (Spencer et al., 2012). Jiang et al. (2012) also examined the relationship between DOC and CDOM for Lake Taihu, and found that a relative stable relationship was observed for water samples collected in different seasons except those measured in winter. Further, obvious seasonal variations were observed, which could be explained by the mixing of various endmembers of CDOM originated from different types of terrestrial ecosystems and internal source as well (Zhang et al., 2010; Spencer et al., 2012).

As argued by Tranvik et al. (2009) and Raymond et al. (2013), remote sensing technology was supposed to play a vital role in quantification of inland waters for carbon cycling. To date, various attempts have been made to characterize DOC and CDOM for both oceanic and inland waters and assess the relationship between these

Hydrol. Earth Syst. Sci. Discuss., doi:10.5194/hess-2016-380, 2016
Manuscript under review for journal Hydrol. Earth Syst. Sci.
Published: 22 August 2016

two forms of carbons (Vodacek et al., 1999; Fichot and Benner, 2011; Griffin et al., 2011; Spencer et al., 2012; Zhu et al., 2013). However, the variation for this relationship with various types of inland waters, especially saline water and urban water bodies were not examined in depth. In this study, the characteristics of DOC and CDOM within different types of inland waters across China were examined to determine its spatial feature associated with landscape variations, hydrologic conditions and saline gradients. To specific, the objectives of this study are to: 1) examine the relationship between CDOM and DOC concentrations across a wide range of waters with various physical, chemical and biological conditions, 2) compare the behavior of the relationships between DOC and CDOM for various water types, and 3) establish model for the relationship between DOC and CDOM based on the sorted CDOM absorption features, e.g., SUVA254 and the ratio of a_{250} : a_{365} (DeHaan, 1993; Weishaar et al., 2003). To address these objectives, 1504 water samples were collected in fresh and saline water lakes, reservoirs, rivers and streams, ponds across China that encompass a broad ranges of DOC, CDOM concentrations with various natural conditions, e.g., temperature, precipitation, hydrology, morphology, soil type and landscape gradients. The findings from this research is essential for understanding the relationship between DOC and CDOM with various types of inland waters, which set a bridge for remote estimation of DOC contained in lakes or reservoirs.

2. Materials and Methods

The dataset is composed of five subsets of samples collected from various types of waters across China (Table 1), which encompassed a wide range of DOC and CDOM

Hydrol. Earth Syst. Sci. Discuss., doi:10.5194/hess-2016-380, 2016
Manuscript under review for journal Hydrol. Earth Syst. Sci.
Published: 22 August 2016

originating from different sources. The first dataset (n = 288; from early spring 2009 to late October 2014) was measured from samples collected in fresh lakes and reservoirs for describing variations in absorption properties of different CDOM and DOC sources during the growing season with various landscape types. The second dataset (n = 345; from early spring 2010 to late mid-September 2014) was measured from samples collected in brackish to saline water bodies for investigating variations in CDOM absorption properties and hydrological impact on DOC concentration. The third dataset (n =322; from early May 2012 to late October 2014) was measured from samples collected in rivers and streams across a wide region in China. The fourth data (n = 328; from 2011 to 2014 in the ice frozen season) was measured from samples collected in northeast China in winter from both lake ice and underlying waters. The fifth dataset (n = 221; from early May 2013 to mid-October 2014) was measured of samples from urban water bodies, including lakes, ponds, rivers and streams, which was severely influenced by sewage effluents. It is expected that CDOM and DOC from various water types may illustrate a general trend between these two parameters.

[Insert Fig.1 about here]

2.1 Water quality determination

In the laboratory, water salinity was measured through DDS-307 electrical conductivity (EC) meter (μS/cm) at room temperature (20±2℃) and transformed to practical salinity units (PSU). Water samples were filtered and extracted with acetone for chlorophyll-a (Chl-a) concentration determination using a Shimadzu UV-2050PC

Hydrol. Earth Syst. Sci. Discuss., doi:10.5194/hess-2016-380, 2016
Manuscript under review for journal Hydrol. Earth Syst. Sci.
Published: 22 August 2016

spectrophotometer (Song et al., 2013). Total suspended matter (TSM) was determined gravimetrically, details can be found in Song et al. (2013). DOC concentrations were determined by high temperature combustion (HTC) with water samples filtered through pre-combusted 0.45 μm GF/F filters (Song et al., 2013). The standards for dissolved total carbon (DTC) were prepared from reagent grade potassium hydrogen phthalate in ultra-pure water, while dissolved inorganic carbon (DIC) were determined using a mixture of anhydrous sodium carbonate and sodium hydrogen carbonate. DOC was calculated by subtracting DIC from DTC, both of which were measured by a Total Organic Carbon Analyzer (Shimadzu, TOC-VCPN). Total nitrogen (TN) was measured based on the absorption levels at 146 nm of water samples decomposed with alkaline potassium peroxydisulfate. Total phosphorus (TP) was determined using the molybdenum blue method after the samples were digested with potassium peroxydisulfate (APHA, 1998). A PHS-3C pH meter was used to determine pH at room temperature (20±2 ℃) in laboratory.

2.2 CDOM absorption and spectral slope (S) derivation

First, all the samples were filtered at low pressure, first through a pre-combusted Whatman GF/F filter (0.7μm) in the laboratory, and then the filtrate were further filtered through pre-rinsed 25 mm Millipore membrane cellulose filter (0.22 μm) at a low pressure. Absorption spectra were obtained between 200 and 800 nm at 1 nm increment using a Shimadzu UV-2600PC UV-Vis (Shimadzu Inc., Japan) dual beam spectrophotometer through a 1 cm quartz cuvette (or 5 cm cuvette for ice melted

Hydrol. Earth Syst. Sci. Discuss., doi:10.5194/hess-2016-380, 2016
Manuscript under review for journal Hydrol. Earth Syst. Sci.
Published: 22 August 2016

Hydrology and Earth System Sciences
Discussions

155 water samples), and Milli-Q water was used as reference for CDOM absorption
156 measurements. The absorption coefficient (a_{CDOM}) was calculated from the measured
157 optical density (*OD*) of samples using Eq. (1):

158 $$a_{CDOM}(\lambda) = 2.303[OD_{S(\lambda)} - OD_{(null)}]/\beta \quad (1)$$

159 where β is the cuvette path length (0.01 or 0.05m) and 2.303 is the conversion factor
160 of base 10 to base *e* logarithms. To remove the scattering effect from fine particles
161 remained in the filtered solutions, a necessitated correction was implemented. The
162 $OD_{(null)}$ is the average optical density over 740–750 nm, which is assumed to be zero
163 for the absorbance of CDOM (Zhang et al., 2007). All absorption measurements were
164 conducted within 48 h after the samples were shipped back to the laboratory. The
165 specific CDOM absorption coefficients were calculated as the ratio of $a_{CDOM}(\lambda)$
166 against DOC concentration, and denoted as $a^*_{CDOM}(\lambda)$ with units of (m^{-1}.L.mg^{-1}). In
167 the current study, the value of $a^*_{CDOM}(\lambda)$ at reference wavelength of 350 nm was
168 calculated as suggested by previous investigations (Vodacek et al., 1999; Fichot and
169 Benner, 2011), which will be further used as spectral index for establishing
170 relationship between CDOM and DOC.

171 A CDOM absorption spectrum, $a_{CDOM}(\lambda)$, is generally expressed as an
172 exponential function (Babin et al., 2003):

173 $$a_{CDOM}(\lambda_i) = a_{CDOM}(\lambda_r)e^{-S(\lambda_i - \lambda_r)} \quad (2)$$

174 where $a_{CDOM}(\lambda_i)$ is the CDOM absorption at a given wavelength λ_i, $a_{CDOM}(\lambda_r)$ is the
175 absorption estimate at the reference wavelength (i.e., λ_r = 440 nm) and *S* is the
176 spectral slope. The *S* is calculated by fitting the data to a nonlinear model over a

Hydrol. Earth Syst. Sci. Discuss., doi:10.5194/hess-2016-380, 2016
Manuscript under review for journal Hydrol. Earth Syst. Sci.
Published: 22 August 2016

177 wavelength range of 300 to 500 nm as suggested by Zhang et al. (2007).

178 ## 3. Results and discussion

179 In all datasets collected over different types of water bodies across China, a large
180 diversity of inland waters with varying water qualities was encountered. High average
181 Chl-a concentrations (46.44±59.71 μgL^{-1}) are observed in these waters, which ranged
182 between 0.28-521.12 μg/L. As shown in Table 1, fresh water, saline water and
183 particularly urban water bodies all exhibited high TN and TP values, indicating that
184 most of the waters are highly eutrophic. It should be noted that even winter water
185 samples also revealed high Chl-a concentration (7.3±19.7 μgL^{-1}), which is resulted
186 from high TN (4.3±5.4mgL^{-1}) and TP (0.7±0.6mgL^{-1}) concentrations even under ice
187 covered conditions. Due to regional hydro-geologic and climatic conditions, most
188 waters in the semi-arid and arid regions have high electric conductivity (EC:
189 1067-41000 μs/cm) and pH values (7.1-11.4). Overall, waters are highly turbid by
190 showing high concentration of TSM (119.55 ± 131.37 mgL^{-1}), but different water
191 types demonstrated obvious variations in the water column (Table 1). Hydrographic
192 conditions exert strong impact on water turbidity and TSM concentration, thus these
193 two parameters for river and stream samples were not measured in this study (Table 1).
194 Large variations of water quality parameters extensive geographic conditions set a
195 more representative basis for examination of the relationship between DOC and
196 CDOM, which is potentially helpful for remote estimate of DOC through CDOM
197 absorption properties (Kutser et al., 2015).

198 **[Insert Table 1 about here]**

Hydrol. Earth Syst. Sci. Discuss., doi:10.5194/hess-2016-380, 2016
Manuscript under review for journal Hydrol. Earth Syst. Sci.
Published: 22 August 2016

3.1. DOC concentrations in various types of waters

The range of DOC concentrations spanned an order of magnitude over these waters being investigated. As shown in Table 1, low averaged concentration of DOC was observed for river waters, but even lower DOC concentrations were measured with ice melting waters sampled in winter. It should be noted that large variations were measured with waters from rivers and streams (Table 2). Generally, low DOC concentrations were found in rivers or streams in the drainage systems developed in Tibetan Plateau or arid regions where soil contains relative low concentration of soil organic carbon, while inverse trend were found in rivers or streams surrounded by forest or wetlands. Among the five types of waters investigated, high DOC concentrations were recorded for saline waters, ranging from 2.3 to 300.6 mg/L. This investigation indicated that saline waters originated from the Songnen Plain, the HulunBuir Plateau and part of waters from Tibetan Plateau generally exhibits high concentration of DOC, while some of waters supplied with snow melt water or ground waters generally exhibit low DOC concentrations even with high salinity. Compared with samples collected in growing seasons, higher DOC concentrations were observed in ice covered water bodies (7.3-720 mg/L), which is due to the condensed effect caused by the DOC expelled from ice formation (Bezilie et al., 2002). This condensed effect is particularly marked for these shallow water bodies, where ice forming remarkably condensed the DOC in the underlying waters (Zhao et al., 2016). As shown in Table 2, even in river or saline water bodies, the concentrations of DOC demonstrated obvious variations. Comparatively, river waters from Qinghai exhibited

Hydrol. Earth Syst. Sci. Discuss., doi:10.5194/hess-2016-380, 2016
Manuscript under review for journal Hydrol. Earth Syst. Sci.
Published: 22 August 2016

lower DOC concentration, while these from Liaohe and Inner Mongolia showed much higher concentration. Likewise, large variations were exhibited for saline waters of different regions (Table 2). Saline waters from the Qinghai and Hulunbir showed much higher DOC concentration, while these from the Xilinguole Plateau and the Songnen Plain exhibited relative lower DOC concentrations.

[Insert Table 2 about here]

3.2. DOC versus CDOM with various types of waters

3.2.1 Fresh waters

The relationships between DOC and CDOM have been examined based on CDOM absorption spectra at different wavelength (Fichot and Benner, 2011; Spencer et al., 2012). As suggested by Fichot and Benner (2011), CDOM absorptions at 275 nm (CDOM275) and 295 nm have stable performances for DOC estimates. As shown in Fig.2a, a strong relationship (R^2 = 0.85) between DOC and CDOM275 was exhibited with samples collected in fresh lakes and reservoirs. Regression analyses of the dataset collected from different regions indicated that the slope values varied from 1.87 to 3.22. The results indicated that water samples from North China and East China turned to have lower regression slope values, where lakes and reservoirs generally ranged from mesotrophic to eutrophic status. Phytoplankton degradation may contribute relative large portion of DOC in these water bodies (Zhang et al., 2010). Comparatively, fresh water bodies from Northeast China revealed larger regression slope values, and CDOM from these water bodies are surrounded by forest, wetlands and grassland generally exhibit high proportion of colored fractions (Helms

Hydrol. Earth Syst. Sci. Discuss., doi:10.5194/hess-2016-380, 2016
Manuscript under review for journal Hydrol. Earth Syst. Sci.
Published: 22 August 2016

et al., 2008). Further, soils in Northeast China are endorsed with high organic carbon, which may also contribute high concentration of DOC and CDOM in waters from this region (Jin et al., 2016). Compared with waters from East and South China, water bodies in Northeast China show less algal bloom due to the low temperature, thus autochthonous CDOM is less presented in waters from Northeast China (Song et al., 2013; Zhao et al., 2016).

3.2.2 Saline lakes

As shown in Fig.2b, a strong relationship (R^2 = 0.85) between DOC and CDOM275 was demonstrated for saline waters. However, compared to fresh waters, much lower regression slope value (slope = 1.28) was exhibited for saline waters. Similar to fresh water bodies, the slope values for most saline waters exhibited large variations from different regions, ranging from 0.67 to 2.47. As the extreme case, the slope value is only 0.33 as demonstrated in the embedded diagram in Fig.2b. Our analyses indicated that the saline waters from semi-arid or arid regions, e.g., west Songnen Plain (2.47), Hulunbir Plateau and East Inner Mongolia Plateau (1.79) generally exhibit higher regression slope values. Whereas, water bodies from the western part of Inner Mongolia Plateau (1.13), the Tibetan Plateau (0.86) exhibited low slope values, and the extreme low value was measured with the Lake Qinhai from Tibetan Plateau, and lakes from Tarim Basin, where lakes experience long resident time and strong solar radiation enhances the photo-bleaching effects (Spencer et al., 2012; Song et al., 2013; Wen et al., 2016). Thereby, less colored portion of DOC was presented in water bodies in semi-arid to arid regions, especially for these closed lakes with enhanced

Hydrol. Earth Syst. Sci. Discuss., doi:10.5194/hess-2016-380, 2016
Manuscript under review for journal Hydrol. Earth Syst. Sci.
Published: 22 August 2016

photochemical processes resulting in lower regression slope value (Spencer et al., 2012). The findings highlighted that remote sensing of DOC through CDOM absorption algorithm for saline waters was remarkably different from fresh waters.

3.2.3 Stream and rivers

Though some of the samples scattered from the regression line (Fig.2c), close relationship between DOC and CDOM275 was revealed for samples collected in rivers and streams. Compared with the other water types (Fig.2), the highest regression slope value (slope = 3.13) was exhibited with river and stream water samples. Further regression analysis with sub-datasets measured with water samples collected in different regions indicated that slope values presented large variability, ranging from 1.84 to 8.41. The lower regression slope was recorded with water samples collected in rivers and stream in semi-arid and arid regions, e.g., the Tibetan Plateau, Mongolia Plateau and Tarim Basin, while the higher values were found with samples collected in streams originated from wetland and forest in Northeast China. Rivers and streams in North, East and South China generally exhibit intermediate value, ranging from 2.5 to 4.2. In addition, large river water generally presented relatively low slope value, streams, especially head water originating from forest and wetland dominated regions show higher regression slope value, which is consistent with the finding from Helm et al. (2008) and Spencer et al. (2012). In fact, landscape pattern in a specific watershed, including soil organic carbon, may be important factors governing the terrestrial DOC and CDOM characteristics in rivers and streams encompassed in the watershed (Wilson and Xenopoulos, 2008; Jaffe et al., 2008).

Hydrol. Earth Syst. Sci. Discuss., doi:10.5194/hess-2016-380, 2016
Manuscript under review for journal Hydrol. Earth Syst. Sci.
Published: 22 August 2016

287 ***3.2.4 Urban waters***

288 Although close relationship between DOC and CDOM275 was revealed with urban
289 waters (Fig.2d, R^2 = 0.71), it is much scattered compared with other water types
290 (Fig.2), particularly with samples presenting DOC concentration less than 60 mg/L.
291 Similarly, very large variability of regression slope values was demonstrated, ranging
292 from 0.78 to 4.16. It is apparent that urban water bodies are severely affected by
293 human activities, particularly sewage, effluents and runoff from urban impervious
294 surface containing large amount of DOM and nutrient discharge into urban waters.
295 Elevated nutrients generally result in algal bloom for some of the urban water bodies
296 (Chl-a range: 1.0-521.1 μg/L; average: 38.9 μg/L). Thereby, DOC and CDOM derived
297 from phytoplankton may also contribute a portion that should not be neglected (Zhao
298 et al., 2016; Zhang et al., 2010). More or less affected by sewage effluent, the DOM
299 in urban waters is much complex than those from natural water bodies. Thus, a large
300 variation of the relationship between DOC and CDOM275 is expected with urban
301 waters.

302 ***3.2.5 Ice covered lakes and reservoirs***

303 As demonstrated in Fig.2e, a closest relationship (R^2 = 0.93) between DOC and
304 CDOM275 was recorded with waters beneath ice covered lakes and reservoirs in
305 Northeast China. It was argued that the close relationship indicated the concurrent
306 processes taken place for DOC accumulation and CDOM biogeochemical activities
307 (Finlay et al., 2003; Stedmon et al., 2011). The strong positive correlations between
308 DOC and CDOM275 is probably due to ice formation condensed these two

Hydrol. Earth Syst. Sci. Discuss., doi:10.5194/hess-2016-380, 2016
Manuscript under review for journal Hydrol. Earth Syst. Sci.
Published: 22 August 2016

parameters. The other possible explanation is that ice and snow cover shield out most of the solar radiation that may cause a series of biochemical process for CDOM contained in water, the inflows and direct rainfall over lakes or reservoirs also diminished, thus causing limited effect on DOC concentration and CDOM composition (Uusikiv et al., 2010; Belzile et al., 2002). Further, the autochthonous DOC and CDOM for ice covered waters are also very limited due to the weak primary production in winter (7.3μg/L). Thus, much close relationship between DOC and CDOM is expected for winter waters.

Comparatively, a loose correlation between DOC and CDOM275 was demonstrated for ice melting waters (Fig.2f) are probably due to the ice/water depth ratio, which cause variation of dissolved components expelled during ice formation. The other reason is probably due to the biologically derived DOC in the ice matrix, which could be varied due to the light and nutrient conditions (Arrigo et al., 2010; Muller et al., 2011). Apparently, CDOM from ice melting waters were mainly originated from maternal water during the ice formation, also from algal biological processes (Stedmon et al., 2009; Arrigo et al., 2010). The DOC and CDOM concentrations in maternal waters, and ice formation processes may cause the variations for their relationship, thus the regression slopes varies. Similarly, snow cover, and nutrients in the ice also cause the variation for biochemical processes, that ultimately result in the relationship between DOC and CDOM may differ from corresponding waters (Bezilie et al., 2002; Spencer et al., 2009). Interestingly, the regression slopes for ice samples (slope = 1.35) and under lying water sample (slope =

Hydrol. Earth Syst. Sci. Discuss., doi:10.5194/hess-2016-380, 2016
Manuscript under review for journal Hydrol. Earth Syst. Sci.
Published: 22 August 2016

1.27) are very close, which may also explain that the dominant components of CDOM and DOC in the ice are from maternal underlying waters.

[Insert Fig.2 about here]

3.3 DOC versus CDOM based on SUVA254 and M (a_{250}:a_{365}) values

Through comparison of the relationships between DOC and CDOM275, it can be seen that the regression slope vales exhibit large variability for various types of waters. The underlying reasons may lies in the aromacity and colored fractions in DOC component (Spencer et al., 2009, 2012). Since SUVA254 is an effective indicator to characterize CDOM molecular weight, and is calculated by the ratio of CDOM absorption at 254 nm to DOC (Weishaar et al., 2003), it may reflect the regression slope value between DOC and CDOM absorption at 275 nm. As shown in Fig.3a, it is obvious that SUVA254 presented high values for both fresh water bodies, and waters from rivers or streams as well. Saline water and winter water samples show intermediate SUVA254 values, while urban water and ice melting water show lower values. The M value (a_{250} : a_{365}) is another indicator to demonstrate the variation of molecular weight and aromacity of CDOM components (Dehaan, 1993). As shown in Fig.3b, fresh water, river and stream water, and urban water exhibit low values, which indicated that larger aromacity dominant for these three types of waters, whereas saline water, winter water and ice melting water show higher M values. Since, SUVA254 and M values reveal molecular weight and aromacity, it might help to estimate DOC through CDOM absorption based on SUVA254 and M threshold values

Hydrol. Earth Syst. Sci. Discuss., doi:10.5194/hess-2016-380, 2016
Manuscript under review for journal Hydrol. Earth Syst. Sci.
Published: 22 August 2016

for various types of waters being investigated.

[Insert Fig.3 about here]

3.3.1 Regression based on SUVA254 grouping

Based on the threshold value for SUVA254, eight subsets of paired DOC and CDOM275 were grouped. Figs.4a to 4f demonstrated the regressions between DOC and CDOM275 with a SUVA254 increment of unity. Fig.4g and 4h exhibited the cases with SUVA254 threshold larger than unity. Except the regression model with SUVA254 less than one (Fig. 4a), better performances were achieved for regression models based on SUVA254 thresholds between 2 to 6 (Figs.4b-4f). As shown in Fig.4a-4h, as a whole, the regression slope values have strong links with SUVA254 values, i.e., slope values increased with SUVA254 increment except for SUVA254 ranging from 6 to 8. It is still not clear whether it is because some outliers or the complex relationship between SUVA254 and DOC, further investigation is required to figure out the underlying reasons. It can be seen that in most of cases, the regression models performed much better based on SUVA254 thresholds. The less promising cases were related with subset of data with lower and high SUVA254 values, relatively larger variations at inner groups are expected thus outperformed by regression models with intermediate SUVA254 values.

[Insert Fig.4 about here]

3.3.1 Regression based on M value grouping

Likewise, regression models between DOC and CDOM275 were established based on

Hydrol. Earth Syst. Sci. Discuss., doi:10.5194/hess-2016-380, 2016
Manuscript under review for journal Hydrol. Earth Syst. Sci.
Published: 22 August 2016

M threshold values (Fig.5). A relative loose correlation between DOC and CDOM275 was revealed with dataset where M value was less than 5 (Fig.5a). It should be noted that the highest regression slope value was achieved among different groups of subset of data (Figs.5a-5h). The large range of M value ($0<M<5.0$) may explain the scattered data pairs in Fig.5a; similar reason can be ascribed to the group with M value ranging from 4 to 6 (Fig.5b). Better regression models were achieved with intermediate M value groups (Figs.5c-5f), where regression slope values were close to each other (ranging from 1.15 to 1.38) with high determination of coefficients ($R^2 > 0.88$). With increased M values, small regression slope values were obtained (Figs.5g-h). Loose relationship between DOC and CDOM275 was obtained with relative low or high M values (Fig.5g). However, very close relationship ($R^2 = 0.99$) was yielded with extremely high M values (Fig.5h). It can be seen that most of samples are from these presented in embedded diagram in Fig.2b, the limited water bodies in the group may be explain this coincidently high R-square value. With more samples collected from different water bodies in this extreme group, a loose relationship between DOC and CDOM275 may be expected, which also needs future explorations.

As noted in Figs.5c-5f, close regression slope values were obtained, implicating that a comprehensive regression model with intermediate M value groups may be achieved. As expected, a promising regression model (the diagram was not shown) between DOC and CDOM 275 was achieved ($y = 1.269x + 6.55$, $R^2 = 0.925$, $N = 998$, $p < 0.001$) with pooled dataset presenting in Figs.5c to 5f. As shown in Fig.6a, a close relationship between DOC and CDOM 275 was obtained with the pooled dataset (N =

Hydrol. Earth Syst. Sci. Discuss., doi:10.5194/hess-2016-380, 2016
Manuscript under review for journal Hydrol. Earth Syst. Sci.
Published: 22 August 2016

1504) collected from different types of inland waters. However, it should be admitted that the extremely high DOC samples may advantageously contribute the better performance of the regression model. Thus, regression model was established without these eight samples (DOC > 300 mg/L), still acceptable accuracy can be achieved (Fig.6b, R^2 = 0.66, $p < 0.01$). In addition, regression model based on logarithm transformed pool dataset was also established (Fig.6c, R^2 = 0.82, $p < 0.01$). It can be seen that most of the paired data sitting close to the regression line except some scattered ones. Based on the regression analysis on pooled dataset, it can be concluded that it is possible to derive DOC concentration based on CDOM absorption spectra, and the latter parameter can be estimated from remotely sensed data (Zhu et al., 2011; Kuster et al., 2015).

[Insert Fig.5 and Fig.6 about here]

4. Conclusion

As a powerful means, remote sensing plays a crucial role in assessing CDOM and DOC in lake and reservoir waters. However, in order to get accurate estimates of CDOM and DOC in waters, it is necessary to get insight into the regional water optical properties for developing semi-analytical or analytical models with remotely sensed data. Based on CDOM absorption spectral measurements and DOC laboratory analysis, we have investigated the relationships between CDOM and DOC for various water types systematically. The investigation showed that CDOM absorption varied significantly, and generally river waters and fresh lake waters exhibit high CDOM

Hydrol. Earth Syst. Sci. Discuss., doi:10.5194/hess-2016-380, 2016
Manuscript under review for journal Hydrol. Earth Syst. Sci.
Published: 22 August 2016

417 absorption values and specific CDOM absorption (SUVA254) as well. On the contrast,
418 saline waters illustrate low SUVA254 values due to the long residence time and strong
419 photo-bleaching effects on waters in the semi-arid regions. Influenced by effluents
420 and sewage waters, CDOM from urban water bodies showed much complex
421 absorption feature. With respect to ice melting water samples, SUVA254 for CDOM
422 was lowest for all groups of waters concerned.

423 The current investigation indicated that the relationships between CDOM
424 absorption and DOC varied significantly by showing different slope values with
425 various water types of regression models. The slope values for saline and urban
426 waters are close to unity, while river water exhibited highest slope value (~ 3.1) of all
427 water types concerned, and other water types are in between. When all the data set
428 pooled together, the slope for regression model is about 1.3, but with much higher
429 uncertainty (R^2 = 0.66). Regression model accuracy for CDOM275 against DOC was
430 improved when CDOM absorptions were divided into different sub-groups according
431 to SUVA254 or M values (a_{250}:a_{365}). This finding highlights that remote sensing
432 models for DOC estimates based on the relationship between CDOM and DOC need
433 to consider water types or cluster waters into several groups according to their
434 absorption features, ultimately improved model accuracy is expected.

435

436 **Acknowledgements**

437 The authors would like to thank financial supports from Natural Science Foundation
438 of China (No.41471290), and "One Hundred Talents" Program from Chinese

Hydrol. Earth Syst. Sci. Discuss., doi:10.5194/hess-2016-380, 2016
Manuscript under review for journal Hydrol. Earth Syst. Sci.
Published: 22 August 2016

Academy of Sciences granted to Dr. Kaishan Song. Thanks are also extended to all the staff and master students for their efforts in field data collection and laboratory analysis.

References

Arrigo, K.R., Mock, T., and Lizotte, M.P. 2010. Primary producers and sea ice, In *Sea Ice*, edited by D.N. Thomas, and G.S. Dieckmann, pp. 283-326, second ed., Wiley-Blackwell, Oxford, UK.

Belzile, C., Gibson, J.A.E., Vincent, W.F., 2002. Colored dissolved organic matter and dissolved organic carbon exclusion from lake ice: implications for irradiance transmission and carbon cycling. Limnology and Oceanography, 47(5), 1283–1293.

Binding, C.E., John. H. J., Robert. P. B., et al. 2008. Spectral absorption properties of dissolved and particulate matter in Lake Erie. Remote Sensing of Environment, 112(4), 1702-1711.

Bricaud, A., Ciotti, A.M., Gentili, B., 2012. Spatial-temporal variations in phytoplankton size and colored detrital matter absorption at global and regional scales, as derived from twelve years of SeaWiFS data (1998–2009). Global Biogeochemical Cycles, 26, GB1010, doi:10.1029/2010GB003952.

DeHaan, H., 1993. Solar UV-light penetration and photodegradation of humic substances in peaty lake water. Limnology and Oceanography, 1993, 38,

461 1072–1076.

462 Duarte, C.M., Prairie, Y.T., Montes, C., et al. 2008. CO2 emission from saline lakes: A
463 global estimates of a surprisingly large flux. Journal of Geophysical Research,
464 113: G04041.

465 Fellman, J.B., Petrone, K.C., Grierson, F. 2011. Source, biogeochemical cycling, and
466 fluorescence characteristics of dissolved organic matter in an agro-urban estuary.
467 Limnology and Oceanography, 56(1), 243–256.

468 Ferrari, G.M. Tassan, S. 1992. Evaluation of the influence of yellow substance
469 absorption on the remote sensing of water quality in the Gulf of Naples: a case
470 study. International Journal of Remote Sensing, 13, 2177–2189.

471 Ferrari, G. M. & Dowell. M. D. 1998. CDOM absorption characteristics with relation
472 to fluorescence and salinity in coastal areas of the Southern Baltic Sea. Estuarine,
473 Coastal and Shelf Science, 47, 91–105.

474 Fichot, C.G., Benner, R. 2011. A novel method to estimate DOC concentrations from
475 CDOM absorption coefficients in coastal waters. Geophysical Research Letter,
476 38, L03610.

477 Griffin, C.G., Frey, K.E., Rogan, J., Holmes, R.M. 2011. Spatial and interannual
478 variability of dissolved organic matter in the Kolyma River, East Siberia,
479 observed using satellite imagery. Journal of Geophysical Research, 116,
480 G03018.

481 Helms, J.R., Stubbins, A., Ritchie, J.D., Minor, E.C., Kieber, D.J., Mopper, K. 2008.
482 Absorption spectral slopes and slope ratios as indicators of molecular weight,

source, and photobleaching of chromophoric dissolved organic matter. Limnology and Oceanography, 53, 955–969.

Jaffé, R., McKnight, D., Maie, N., Cory, R., McDowell, W.H., Campbell, J.L. 2008. Spatial and temporal variations in DOM composition in ecosystems: The importance of long-term monitoring of optical properties. Journal of Geophysical Research, 113, G04032.

Jin, X.L., Du, J., Liu, H.J., Wang, Z.M., Song, K.S. 2016. Remote estimation of soil organic matter content in the Sanjiang Plain, Northest China: The optimal band algorithm versus the GRA-ANN model. Agricultural and Forest Meteorology, 218, 250–260.

Hoge, F.E., Lyon, P.E. 1996. Satellite retrieval of inherent optical properties by linear matrix inversion of oceanic radiance models: An analysis of model and radiance measurement errors. Journal of Geophysical Research-Oceans, 101(C7): 16631–16648.

Kowalczuk, P., Stedmon. C. A., Markager. S. 2006. Modeling absorption by CDOM in the Baltic Sea from salinity and chlorophyll. Marine Chemistry, 101, 1–11.

Kutser, T., Verpoorter, C., Paavel, B., et al. 2015. Estimating lake carbon fractions from remote sensing data. Remote Sensing of Environment, 157: 138-146.

Larson, J.H., Frost, P.C., Zheng, Z.Y., Johnston, C.A., Bridgham, S.D., Lodge, D.M., Lamberti, A.A. 2007. Effects of upstream lakes on dissolved organic matter in streams. Limnology and Oceanography, 52(1), 60–69.

Le, C.F., Hu, C.M., Cannizzaro, J., Duan, H.T. 2013. Long-term distribution patterns

505 of remotely sensed water quality parameters in Chesapeake Bay. Estuarine,
506 Coastal and Shelf Science, 128(10), 93–103.
507 Jiang, G.J., Ma, R.H., Duan, H.T. 2012. Estimation of DOC Concentrations Using
508 CDOM Absorption Coefficients: A Case Study in Taihu Lake. Environmental
509 Sicences, 33(7), 2235–2243.
510 Markager, W., Vincent. W. F. 2000. Spectral light attenuation and absorption of UV
511 and blue light in natural waters. Limnology and Oceanography, 45(3), 642–650.
512 Miller, W.L., Zepp, R.G. 1995. Photochemical production of dissolved inorganic
513 carbon from terrestrial organic matter: Significance to the oceanic organic
514 carbon cycle. Geophysical Research Letter, 22 (4), 417–420.
515 Neff, J.C., Finlay, J.C., Zimov, S.A., Davydov, S.P., Carrasco, J.J., Schuur, E.A.G.,
516 Davydova, A.I. 2006. Seasonal changes in the age and structure of dissolved
517 organic carbon in Siberian rivers and streams. Geophysical Research Letter, 33,
518 L23401.
519 Nelson, N.B., Siegel, D.A., Carlson, C.A., Swan, C.M., 2010. Tracing global
520 biogeochemical cycles and meridional overturning circulation using
521 chromophoric dissolved organic matter. Geophysical Research Letter, 37,
522 L03610, doi:10.1029/2009GL042325.
523 Para, J., Coble, P.G., Charriere, B., Tedetti, M., Fontana, C., Sempere, R. 2010.
524 Fluorescence and absorption properties of chromophoric dissolved organic
525 matter (CDOM) in coastal surface waters of the northwestern Mediterranean Sea,
526 influence of the Rhone River. Biogeosciences, 7, 4083–4103.

Hydrol. Earth Syst. Sci. Discuss., doi:10.5194/hess-2016-380, 2016
Manuscript under review for journal Hydrol. Earth Syst. Sci.
Published: 22 August 2016

527 Stedmon, C.A., Thomas, D.N., Papadimitriou, S., Granskog, M.A., Dieckmann, G.S.
528 2011. Using fluorescence to characterize dissolved organic matter in Antarctic
529 sea ice brines. Journal of Geophysical Research, 116, G03027.
530 Spencer, R.G.M., Stubbins, A., Hernes, P.J., Baker, A., Mopper, K., Aufdenkampe,
531 A.K., Dyda, R.Y., Mwamba, V.L., Mangangu, A.M., Wabakanghanzi, J.N., Six, J.
532 2009. Photochemical degradation of dissolved organic matter and dissolved
533 ligninphenols from the Congo River. Journal of Geophysical Research, 114,
534 G03010.
535 Spencer, R.G.M., Butler, K.D., Aiken, G.R. 2012. Dissolved organic carbon and
536 chromophoric dissolved organic matter properties of rivers in the USA. Journal
537 of Geophysical Research, 117, G03001.
538 Song, K. S., Zang, S. Y., Zhao, Y., Li, L., Du, J., Zhang, N. N., Wang, X. D., Shao, T.
539 T., Liu, L., Guan, Y. 2013. Spatiotemporal characterization of dissolved Carbon
540 for inland waters in semi-humid/semiarid region, China. Hydrology and Earth
541 System Science, 17, 4269–4281.
542 Tranvik, L.J., Downing, J.A.,Cotner, J.B., et al. 2009. Lakes and reservoirs as
543 regulators of carbon cycling and climate. Limnology and Oceanography, 54(6),
544 2298–2314.
545 Uusikiv, J., Vahatal, A.V., Granskog, M.A., Sommaruga, R., 2010. Contribution of
546 mycosporine-like amino acids and colored dissolved and particulate matter to
547 sea ice optical properties and ultraviolet attenuation. Limnology and
548 Oceanography, 55(2), 703–713.

Hydrol. Earth Syst. Sci. Discuss., doi:10.5194/hess-2016-380, 2016
Manuscript under review for journal Hydrol. Earth Syst. Sci.
Published: 22 August 2016

549 Verpoorter, C., Kutser, T., Seekell, D.A., Tranvik, L.J. 2014. A global inventory of
550 lakes based on high-resolution satellite imagery. Geophysical Research Letter,
551 41,6396–6402.
552 Vodacek, A., Blough, N.V., Degrandpre, M.D., Peltzer, E.T., Nelson, R.K. 1997.
553 Seasonal variation of CDOM and DOC in the Middle Atlantic Bight: terrestrial
554 inputs and photooxidation. Limnology and Oceanography, 42, 674–686.
555 Weishaar, J.L., Aiken, G.R., Bergamaschi, B.A., Fram, M.S., Fugii, R., Mopper, K.
556 2003. Evaluation of specific ultraviolet absorbance as an indicator of the
557 chemical composition and reactivity of dissolved organic carbon.
558 Environmental Science and Technology, 37, 4702–4708.
559 Wen, Z.D., Song, K.S., Zhao, Y., Du, J., Ma, J.H. 2016. Influence of environmental
560 factors on spectral characteristic of chromophoric dissolved organic matter
561 (CDOM) in Inner Mongolia Plateau, China. Hydrology and Earth System
562 Sciences, 20, 787–801.
563 Williamson, C.E., Rose, K.C. 2010. When UV meets fresh water. Science, 329,
564 637–639.
565 Wilson, H., Xenopoulos, M.A. 2008. Ecosystem and seasonal control of stream
566 dissolved organic carbon along a gradient of land use. Ecosystems 11, 555–568.
567 Yu, Q., Tian, Y, Q., Chen, R.F., Liu, A., Gardner, G.B., Zhu, W.N. 2010. Functional
568 linear analysis of in situ hyperspectral data for assessing CDOM in
569 rivers. Photogrammetric Engineering & Remote Sensing, 76(10), 1147–1158.
570 Zhang, Y.L., Qin, B.Q., Zhu, G.W., Zhang, L., Yang, L.Y. 2007. Chromophoric

Hydrol. Earth Syst. Sci. Discuss., doi:10.5194/hess-2016-380, 2016
Manuscript under review for journal Hydrol. Earth Syst. Sci.
Published: 22 August 2016

571 dissolved organic matter (CDOM) absorption characteristics in relation to
572 fluorescence in Lake Taihu, China, a large shallow subtropical lake.
573 Hydrobiologia, 581, 43–52.
574 Zhang, Y.L., Zhang, E.L., Yin, Y., Van Dijk, M.A.,Feng, L.Q., Shi, Z.Q., Liu, M.L.,
575 Qin, B.Q. 2010. Characteristics and sources of chromophoric dissolved organic
576 matter in lakes of the Yungui Plateau, China, differing in trophic state and
577 altitude. Limnology and Oceanography, 55(6), 2645–2659.
578 Zhao, Y., Song, K.S., Wen, Z.D., Li, L., Zang, S.Y., Shao, T.T., Li, S.J., Du, J. 2016.
579 Seasonal characterization of CDOM for lakes in semiarid regions of Northeast
580 China using excitation–emission matrix fluorescence and parallel factor
581 analysis (EEM‐PARAFAC). Biogeosciences, 13, 1635–1645.
582 Zhu, W., Yu, Q., Tian, Y. Q., et al. 2011. Estimation of chromophoric dissolved
583 organic matter in the Mississippi and Atchafalaya river plume regions using
584 above-surface hyperspectral remote sensing. Journal of Geophysical Research:
585 Oceans (1978–2012), 116(C2), C02011.
586
587
588
589
590
591
592

Hydrol. Earth Syst. Sci. Discuss., doi:10.5194/hess-2016-380, 2016
Manuscript under review for journal Hydrol. Earth Syst. Sci.
Published: 22 August 2016

Hydrology and Earth System Sciences
Discussions

593 **Figures**

594 Fig.1. Water types and sample distributions across the mainland of China.

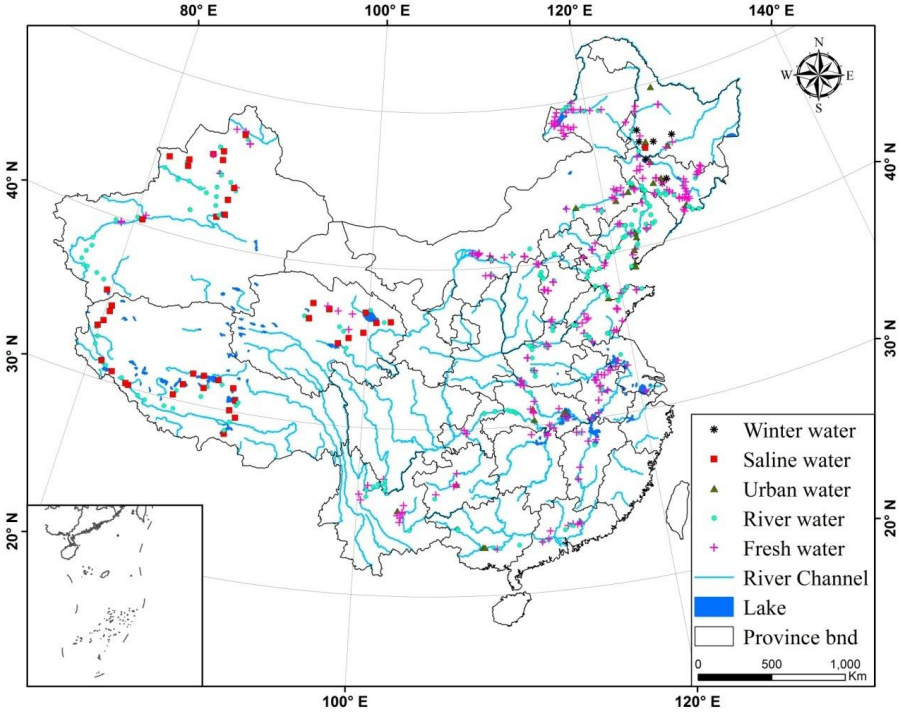

595
596
597
598
599
600
601
602
603
604
605
606
607
608
609
610
611
612
613
614

Hydrol. Earth Syst. Sci. Discuss., doi:10.5194/hess-2016-380, 2016
Manuscript under review for journal Hydrol. Earth Syst. Sci.
Published: 22 August 2016

Hydrology and Earth System Sciences
Discussions

615 Fig.2. Fitting equations of DOC against CDOM275 for different types of inland
616 waters, (a) samples from fresh water lakes, (b) samples from saline water lakes, (c)
617 samples from river waters, (d) samples from urban waters, (e) samples from ice
618 covered waters, and (f) samples from ice melting waters.
619

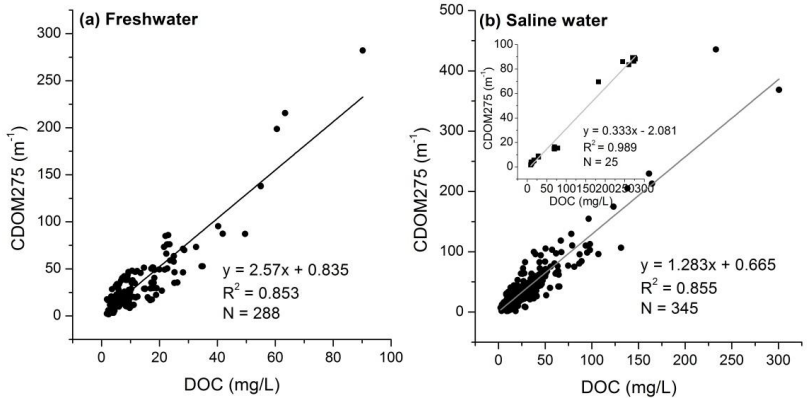

620
621

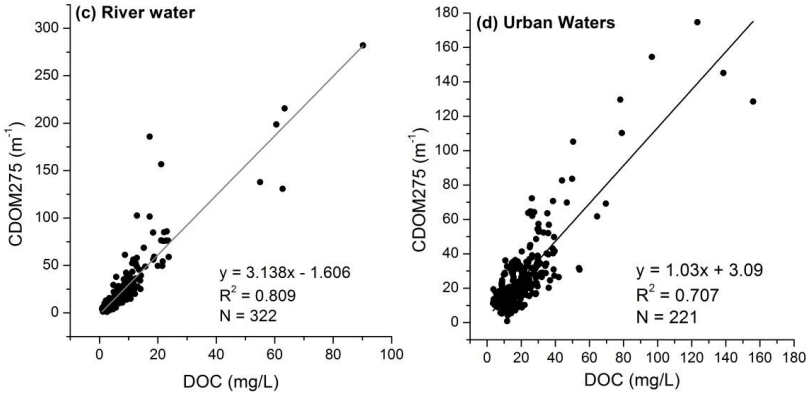

622

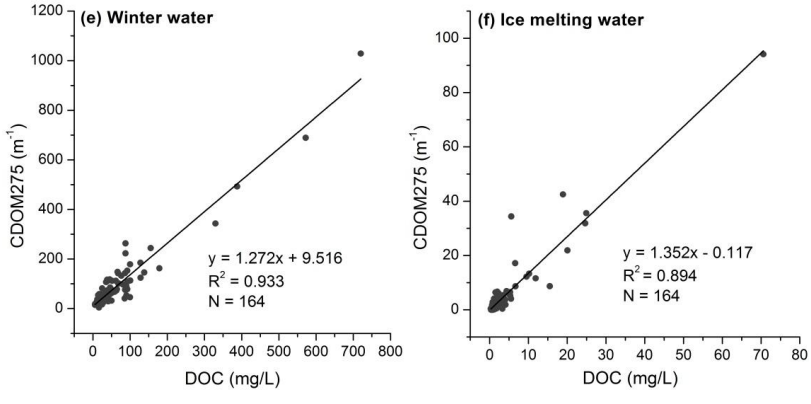

623

Hydrol. Earth Syst. Sci. Discuss., doi:10.5194/hess-2016-380, 2016
Manuscript under review for journal Hydrol. Earth Syst. Sci.
Published: 22 August 2016

Hydrology and Earth System Sciences
Discussions
Open Access
EGU

624 Fig.3. Comparison of (a) SUVA254, and (b) M (a_{250}:a_{365}) values for various types of
625 inland waters. FW, fresh lake water; SW, saline lake water, RW, river or stream water;
626 UW, urban water; WW, winter water from Northeast China; IMW, ice melt water from
627 Northeast China.

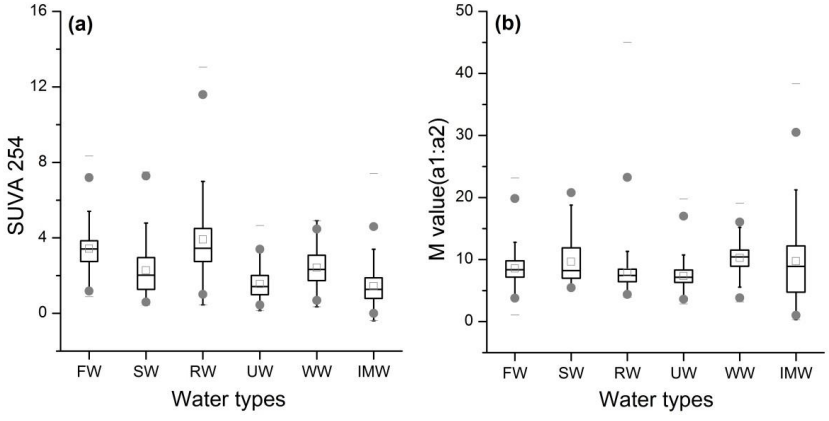

628
629
630
631
632
633
634
635
636
637
638
639
640
641
642
643
644
645
646
647
648
649
650
651
652
653

Hydrol. Earth Syst. Sci. Discuss., doi:10.5194/hess-2016-380, 2016
Manuscript under review for journal Hydrol. Earth Syst. Sci.
Published: 22 August 2016

Hydrology and Earth System Sciences
Discussions

654 Fig.4. Regression models for DOC estimation via CDOM 275 sorted by SUVA254
655 ranges, (a) SUVA254 > 1.0, (b) 1.0 < SUVA254 < 2.0, (c) 2.0 < SUVA254 < 3.0, (d)
656 3.0 < SUVA254 < 4.0, (e) 4.0 < SUVA254 < 5.0, (f) 5.0 < SUVA254 < 6.0, (g) 6.0 <
657 SUVA254 < 8.0, and (h) 8.0 < SUVA254 < 13.1
658
659
660

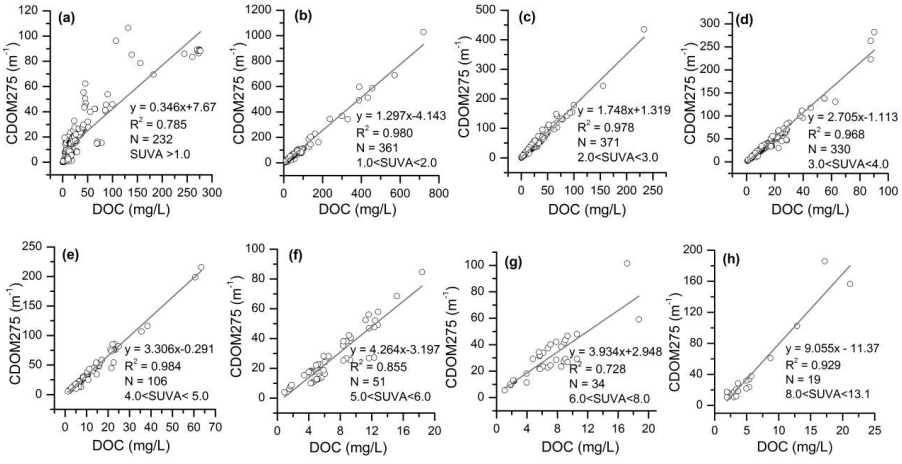

661
662
663
664
665
666
667
668
669
670
671
672
673
674
675
676
677
678
679
680
681
682
683

Hydrol. Earth Syst. Sci. Discuss., doi:10.5194/hess-2016-380, 2016
Manuscript under review for journal Hydrol. Earth Syst. Sci.
Published: 22 August 2016

Hydrology and Earth System Sciences
Discussions

Fig.5. Regression models for DOC estimation via CDOM 275 sorted by M (a1:a2: CDOM250:CDOM365) values ranges, (a) M < 5.0, (b) 4.0 < M< 6.0, (c) 6.0 < M< 6.0, (d) 7.0 < M< 8.0, (e) 8.0 < M< 10.0, (f) 10.0 < M< 12.0, (g) 12.0 < M< 20.0, and (h) 20.0 < M< 68.0.

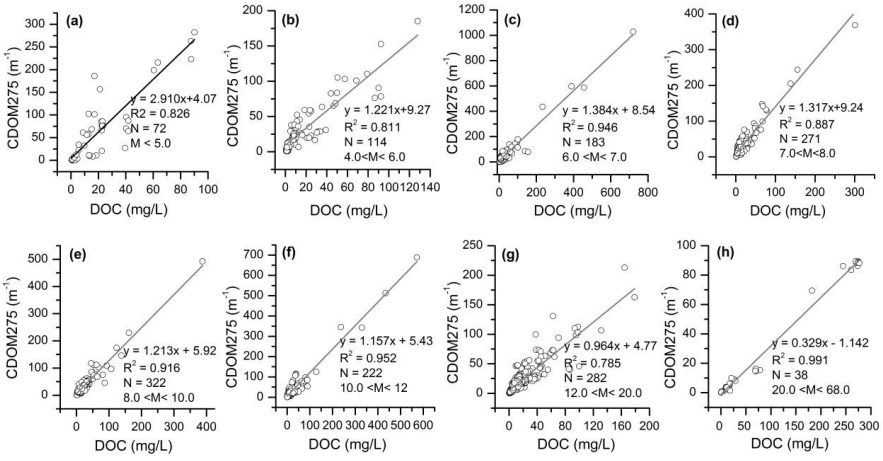

Hydrol. Earth Syst. Sci. Discuss., doi:10.5194/hess-2016-380, 2016
Manuscript under review for journal Hydrol. Earth Syst. Sci.
Published: 22 August 2016

Hydrology and Earth System Sciences
Discussions
Open Access
EGU

714 Fig.6. Relationship between CDOM 275 and DOC concentration. (a) regression
715 model with pooled dataset; (b) regression model with DOC concentration less than
716 300 mg/L; (c) regression model with natural logarithmic transformed data.

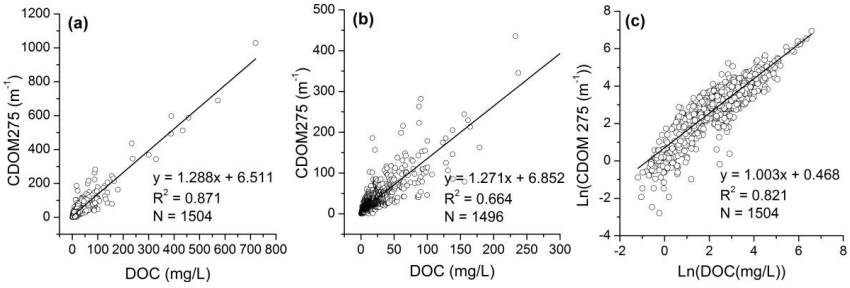

717
718
719
720
721
722
723
724
725
726
727
728
729
730
731
732
733

Hydrol. Earth Syst. Sci. Discuss., doi:10.5194/hess-2016-380, 2016
Manuscript under review for journal Hydrol. Earth Syst. Sci.
Published: 22 August 2016

Hydrology and Earth System Sciences
Discussions
Open Access
EGU

734 **Tables**

735

736 Table 1 descriptive water quality characteristics of different types of waters

		DOC (mg/L)	EC μs/cm	pH	TP (mg/L)	TN (mg/L)	TSM (mg/L)	Chl-a (μg/L)
FW	Mean	10.2	434.0	8.2	0.5	1.6	67.8	78.5
	Range	1.9-90.2	72.7-1181.5	6.9-9.3	0.01-10.4	0.001-9.5	0-1615	1.4-338.5
SW	Mean	27.3	4109.4	8.6	0.4	1.4	115.7	9.0
	Range	2.3-300.6	1067-41000	7.1-11.4	0.01-6.3	0.6-11.0	1.4-2188	0-113.7
RW	Mean	8.3	10489.1	7.8-9.5	--	--	--	--
	Range	0.9-90.2	3.7-1000	8.6	--	--	--	--
UW	Mean	19.44	525.4	8.0	3.4	3.5	50.5	38.9
	Range	3.5-123.3	28.6-1525	6.4-9.2	0.03-32.4	0.04-41.9	1-688	1.0-521.1
WW	Mean	67.0	1387.6	8.1	0.7	4.3	181.5	7.3
	Range	7.3-720	139-15080	7.0-9.7	0.1-4.8	0.5-48	9.0-2174	1.0-159.4
IMW	Mean	6.7	242.8	8.3	0.19	1.1	17.4	1.1
	Range	0.3-76.5	1.5-4350	6.7-10	0.02-2.9	0.3-8.6	0.3-254.6	0.28-5.8

737

738 Note: FW, fresh lake water; SW, saline lake water, RW, river or stream water; UW, urban water;

739 WW, winter water from Northeast China; IMW, ice melt water from Northeast China.

740

741

742

743

744

745

746

747

748

749

750

751

752

753

754

755

756

757

758

759

760

761

Hydrol. Earth Syst. Sci. Discuss., doi:10.5194/hess-2016-380, 2016
Manuscript under review for journal Hydrol. Earth Syst. Sci.
Published: 22 August 2016

Hydrology and Earth System Sciences
Discussions
Open Access
EGU

762 Table 2 descriptive statistics of dissolved organic carbon (DOC) and $a_{CDOM}(440)$ in
763 various types of waters.
764

Type	Region	DOC				$a_{CDOM}(440)$			
		Min	Max	Mean	S.D	Min	Max	Mean	S.D
River	Liaohe	3.6	48.2	14.3	9.49	0.46	3.68	0.92	0.58
	Qinghai	1.2	8.5	4.4	1.96	0.13	2.11	0.54	0.63
	Inner M	16.9	90.2	40.4	24.84	0.32	7.46	1.03	2.11
	Songhua	0.9	21.1	8.1	4.96	0.32	18.93	3.2	4.19
Saline	Qinghai	1.7	130.9	67.9	56.7	0.13	0.86	0.36	0.23
	Hulunbir	8.4	300.6	68.5	69.2	0.82	26.21	4.41	4.45
	Xilinguo	3.74	45.4	14.2	8.8	0.36	4.7	1.34	0.88
	Songnen	3.6	32.6	16.4	7.4	0.46	33.80	2.4	3.78

765
766
767
768
769
770